Thermal Advances 6 (2026) 100119

Contents lists available at ScienceDirect

Thermal Advances

journal homepage: www.elsevier.com/locate/thradv

Full Length Article

Effects of halloysite clay nanotubes on the thermal behaviour of T1107 copolymer

Giuseppe Cavallaro [a,b,*], Maria Vittoria Diamanti [c], Daniela Meroni [b,d], Giuseppe Lazzara [a,b]

[a] Department of Physics and Chemistry Emilio Segrè, Università degli Studi di Palermo. Viale delle Scienze 17, 90128, Palermo, Italy
[b] Consorzio Interuniversitario Nazionale per la Scienza e Tecnologia dei Materiali, INSTM, Via G. Giusti, 9, I-50121 Firenze, Italy
[c] Department of Chemistry, Materials and Chemical Engineering "G. Natta" Politecnico di Milano, Via Mancinelli 7, Milan 20131, Italy
[d] Department of Chemistry, Università degli Studi di Milano, Via Golgi 19, 20133 Milano, Italy

ARTICLE INFO

Keywords:
Halloysite clay nanotubes
T1107 copolymer
Casting procedure
DSC
TGA

ABSTRACT

We have studied the thermal properties of nanocomposites based on T1107 copolymer and halloysite clay nanotubes (HNTs) by combination of Differential Scanning Calorimetry (DSC) and Thermogravimetric Analysis (TGA). Both DSC and TGA experiments have been carried out on T1107/HNTs composites prepared by aqueous casting procedure. The HNTs content has been systematically varied to explore the effect of the composite composition on the thermal characteristic of T1107/halloysite composites. According to DSC results, the presence of HNTs determines a reduction in both temperature and enthalpy of copolymer melting. On the other hand, TGA data have highlighted that the HNTs addition induces destabilization effects on the T1107 resistance to thermal decomposition.

This study shows that the thermal properties of T1107 copolymer are influenced by its interactions with halloysite surfaces, to an extent which depends on the specific composition of the composite materials. T1107/HNTs composites present thermal characteristics suitable for technological and environmental applications, such as adsorption of volatile organic compounds and 3D scaffold for catalysts.

1. Introduction

The combination of clay nanoparticles with polymeric materials represents a powerful strategy to obtain hybrid systems with specific functionalities useful for several purposes, including environmental applications [1–4], biomedicine [5–7] and catalysis [8,9]. Within this, the functionalization of clay nanoparticles with thermo-responsive polymers can be suitable to obtain composite materials with different properties and structure depending on external stimuli, such as temperature variations [10–13]. The adsorption of poly (N-isopropylacrylamide) (PNIPAAM) onto the surfaces of clay nanotubes (imogolite and halloysite) was exploited to prepare thermo-sensitive nanocarriers suitable for drug delivery applications [10,14]. Literature reports that functional composite materials can be fabricated by mixing halloysite clay nanotubes and thermo-responsive copolymers, such as poly(sodium acrylate-acrylamide) (PAA-AM) [15], and blends, including polyacrylic acid (PAA)/polyaniline (PANI) [16]. Recently, halloysite clay nanotubes (HNTs) have been largely employed in a wide range of applications because of their hollow tubular shape and tunable surface properties [17]. Due to their large specific surface, HNTs are efficient catalytic supports [18–20] as well as emulsifying agents for preparation of Pickering emulsions [21–23]. As reported in a recent review [24], HNTs can be used as catalytic supports and nanoreactors/nanotemplates for catalysis due to their surface chemical composition (Si-OH and Al-OH groups). The catalytic performances of halloysite are influenced by different factors, such as temperature and pH conditions, as well as selective modification of inner/outer surfaces. The emulsifying capacity of halloysite depends on its geometrical characteristics (sizes and shape) and wettability, which affect the adsorption free energy at the interface and, consequently, the stability of Pickering emulsions [25]. Moreover, halloysite nanotubes are suitable as nanofillers of polymers for the preparation of nanocomposite films which show promising results for application in packaging and outdoor applications [26–28]. Depending on the chemical structure of polymers, the interactions between halloysite nanotubes and matrix can be driven by supramolecular forces (electrostatic attractions, hydrogen and/or hydrophobic bonds, van der Waals interactions) [29,30], which influence the morphology and the

* Corresponding author.
E-mail address: giuseppe.cavallaro@unipa.it (G. Cavallaro).

https://doi.org/10.1016/j.thradv.2026.100119
Received 8 September 2025; Received in revised form 12 February 2026; Accepted 18 February 2026
Available online 19 February 2026

mesoscopic properties of nanocomposite materials. Literature reports the suitability of HNTs for the fabrication of flame retardant materials [31–33]. Remarkably, halloysite clay is a biocompatible and non-toxic nanomaterial as evidenced by both in-vivo and in-vitro tests [34–36]. Consequently, HNTs can be used for pharmaceutical and biomedical purposes, such as tissue engineering [37–39] and controlled delivery of drug molecules [40–42]. In addition, halloysite is employed in cosmetic formulations for hair treatment and skincare products [25].

The interfacial properties of halloysite are intriguing because of the different chemical composition of inner and outer surfaces. The external surface of HNTs is formed by silicon dioxide (SiO_2), while the cavity is composed by alumina (Al_2O_3). As a consequence of the specific ionization equilibria of SiO_2 and Al_2O_3 groups, inner and outer surfaces present variable charges (positive and negative, respectively) for pH ranging between 4 and 10 [25]. This configuration can be exploited to control the adsorption of ionic macromolecules onto the HNTs surfaces as reported for polymers [43], proteins [44] and surfactants [45]. According to the electrostatic attractions, anionic molecules can be filled within the halloysite cavity, while cationic compounds are proper for the coating of halloysite shell.

In this work, we report for the first time composite materials based on HNTs and Tetronic T1107, which is a positively charged block copolymer suitable for the selective adsorption onto the halloysite outer surface. Tetronics are star block copolymers with four poly(propylene oxide)-poly(ethylene oxide) arms linked to a central ethylene diamine core [46]. Consequently, Tetronics are positively charged macromolecules in a broad range of pH because of the protonation of diamine groups [47]. Literature reports that Tetronics are suitable compounds for numerous applications, which include drug delivery [48–50] and environmental remediation [47,51]. The thermal behavior of T1107 copolymer can be controlled by its interactions with inorganic nanoparticles, such as amorphous TiO_2 [52], as well as by its confinement in the cavity of cyclodextrins [53]. The encapsulation of the copolymer within hydroxypropyl modified cyclodextrins determined a decrease in T1107 crystallinity degree and melting temperature [53].

Thermal investigations are crucial to study supramolecular systems leading to obtain specific information on the interactions between the components [31,32,54–58]. Thermogravimetric analysis (TGA) was successful to explore the electrostatic interactions between poly(vinylidene fluoride) (PVDF) and silanol groups of modified zeolite nanoparticles [59]. Differential Scanning Calorimetry (DSC) and thermogravimetry were employed to investigate the interactions between polyvinyl azide (PVA) and nitrocellulose [60]. Both TGA and DSC allowed to study the supramolecular interactions of T1107 with cyclodextrins [53] and fluorinated surfactants [51].

In this work, TGA and DSC experiments were performed on T1107/HNTs composites to investigate their thermal properties, which are fundamental to evaluate their suitability in environmental and catalytic applications. Moreover, the implementation of DSC and TGA data allowed us to explore the effects of T1107/HNTs interactions on the copolymer melting process and thermal decomposition.

2. Experimental

2.1. Materials

T1107 and HNTs are purchased from Sigma Aldrich. T1107 is a block copolymer $[(EO)_{57}(PO)_{21}]_2NCH_2CH_2N[(PO)_{21}(EO)_{57}]_2$ with a molecular mass of 15,000 g mol^{-1}. The chemical formula of HNTs cell unit is $Al_2SiO_5(OH)_4{\cdot}2H_2O$. The geological source of HNTs is Dragon Mine (Utah, USA), which provided clay samples containing 90 % halloysite with ca. 10 % of kaolinite, quartz and gibbsite [61]. An SEM image of halloysite is presented in Fig. 1. According to literature [24], the length of HNTs is 50–1500 nm, while the inner and outer diameters are 5–30 and 20–150 nm, respectively.

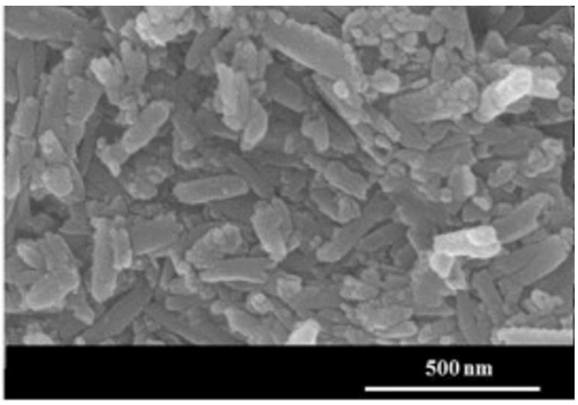

Fig. 1. SEM images of halloysite clay nanotubes from Dragon Mine. Reproduced with copyright permission from [61].

2.2. Preparation of T1107/HNTs composites

The T1107/HNTs composites were prepared using the aqueous casting procedure as reported elsewhere for polymer/halloysite hybrids [62,63]. Firstly, a stable aqueous dispersion of T1107 (concentration of 3.5 wt %) was obtained by magnetically stirring for 2 h at 25 °C. Then, HNTs powder was added to the T1107 dispersion. It should be noted that the amount of halloysite was systematically changed to obtain composite materials with variable T1107/HNTs ratio. The T1107/HNTs aqueous mixture was kept under ultrasonication for 10 min at 25 °C to avoid the formation of halloysite clusters. Finally, the mixture was magnetically stirred overnight at 25 °C allowing to obtain stable dispersions.

The dispersions were poured into glass Petri dishes under vacuum at 25 °C until complete water evaporation. Vacuum conditions enhance water evaporation rate, which is a key factor to improve the uniformity of composite materials. Typically, the casting method for polymer/HNTs nanocomposites is conducted in oven (at temperature > 50 °C) [29], which is not feasible for T1107/HNTs because of the thermosensitive characteristics of the copolymer, which starts to melt at ca. 40 °C. The obtained solid materials (T1107/HNTs composites with variable composition) were stored in desiccator under controlled conditions (relative humidity of 75 % and temperature of 25 °C).

2.3. Methods

2.3.1. Differential scanning calorimetry (DSC)

Differential Scanning Calorimetry (DSC) experiments were conducted using a TA Instruments DSC (2920 CE) under nitrogen atmosphere with a flow rate of 60 cm^3 min^{-1}. The temperature calibration was performed using the melting enthalpy of standard indium (28.71 J g^{-1}) [64]. The samples (ca. 5 mg) were kept in aluminum pans. The measurements were carried out from 10 to 100 °C using the following program: 1) equilibration at 10 °C for 5 min; 2) heating ramp from 10 to 100 °C with a rate of 10 °C min^{-1}; 3) equilibration at 100 °C for 5 min; 4) cooling ramp from 100 to 10 °C with a rate 10 °C min^{-1}. The procedure was repeated twice to evaluate the influence of the thermal history of the samples. DSC data reported in paragraph 3.1 refer to the second cycle of measurements.

2.3.2. Thermogravimetric analysis (TGA)

Thermogravimetric analyses (TGA) were carried out with a Q5000 IR apparatus (TA Instruments). Measurements were performed under nitrogen flow (25 and 10 cm^3 min^{-1} for sample and balance, respectively) from 25 to 600 °C. The heating rate was kept at 10 °C min^{-1}. The measurements were carried out using platinum pans, which contained ca. 4 mg of samples. The temperature calibration of TGA apparatus was

conducted by using the Curie temperatures of standards (nickel, cobalt, and their alloys) as reported elsewhere [65,66].

2.3.3. ζ-potential

ζ-potential measurements were conducted with a Zetasizer Nano-ZS (Malvern Instruments) apparatus. Experiments were carried out at constant temperature ($T = 25$ °C) on aqueous dispersions of HNTs and T1107/HNTs composites using a disposable folded capillary cell. The concentration of the dispersions was fixed at 0.01 wt %.

2.3.4. Scanning electron microscopy (SEM)

The morphology of T1107/HNT composites was studied by Scanning Electron Microscopy (SEM) using an ESEM FEI QUANTA 200F electronic microscope. To avoid charging under the electron beam, each sample was coated with Au in argon by means of an Edwards Sputter Coater S150A. Measurements were conducted in high vacuum mode ($<6 \times 10^{-4}$ Pa) for secondary electrons collection. The energy of the beam was 25 kV and the working distance was 10 mm.

3. Results and discussion

3.1. Thermodynamics of copolymer melting in T1107/HNTs composites

The influence of halloysite addition on T1107 melting was investigated by Differential Scanning Calorimetry. Fig. 2 compares DSC curves of pristine T1107 and the composite filled with 70 % of halloysite. As a general result, we observed an endothermic signal in the range ca. 40–55 °C that can be attributed to the T1107 melting.

The quantitative analysis of the DSC peak allowed to determine the temperature (T_m) and enthalpy variation (ΔH_m) of the melting process for all investigated samples. Specifically, T_m was calculated from the temperature corresponding to the minimum of the DSC signal, while ΔH_m was estimated from the integration of the endothermic peak. Results are reported in Table 1, where ΔH_m values are expressed as Joule per gram of T1107.

We detected that the loading of HNTs induces a decrease in both T_m and ΔH_m in agreement with the presence of specific interactions between T1107 and halloysite surfaces. Table 1 reports the T_m variation (ΔT_m) due to the HNTs addition with respect to pristine T1107. Literature reports similar results for nanocomposites based on HNTs and polyethylene glycols with variable molecular mass [63,67].

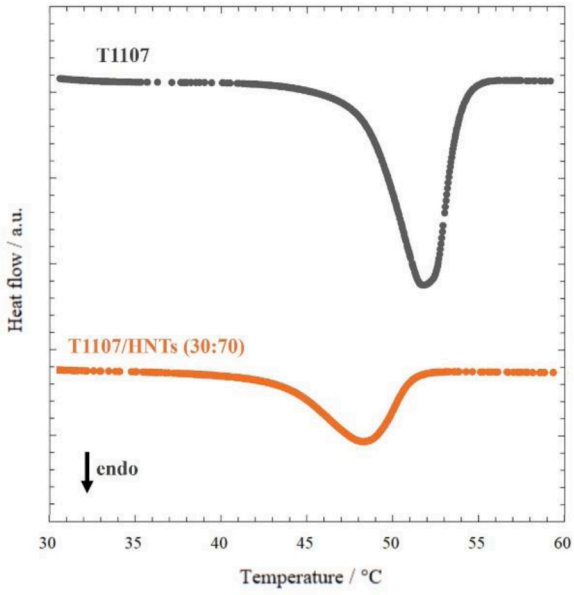

Fig. 2. DSC curves of pristine T1107 and T1107/HNTs (30:70) composite.

Table 1
Temperature and enthalpy of T1107 melting in composite materials with variable composition.

Mass percentage (T1107:HNTs)	T_m / °C	ΔT_m / °C	ΔH_m / J g_{T1107}^{-1}
100:0	52.3		125.9
95:5	52.0	−0.3	118.3
90:10	51.6	−0.7	123.8
75:25	51.2	−1.1	107.3
50:50	48.4	−3.9	96.9
30:70	48.3	−4	90.0
25:75	47.8	−4.5	46.2
15:85	46.7	−5.6	29.3
10:90	46.5	−5.8	23.2
5:95	46.5	−5.8	21.9

The ΔH_m reduction reflects the loss of crystallinity of T1107 copolymer as a consequence of the interactions with HNTs. As reported elsewhere, the relation between the composition of the nanocomposites and the melting enthalpy of polymeric matrices can provide further insights on the interactions between nanofiller and polymer. It is noteworthy that the crystallinity reduction positively influences the T1107 adsorption capacity. As reported in a recent review [68], polymers with a lower crystallinity possess a greater number of adsorption sites for organic pollutants. On the other hand, the loss of T1107 crystallinity can generate a decrease in the mechanical strength because of the random orientation of polymeric chains [69].

Fig. 3 shows the dependence of ΔH_m on the reciprocal of T1107 mass percent (C_{T1107}^{-1}).

We observed an initial linear decrease in ΔH_m that can be attributed to the reduction in copolymer crystallinity. For nanocomposites with a very large HNTs content ($C_{T1107} \leq$ ca. 10 wt %) we detected that ΔH_m is not influenced by variations of composition. According to literature [63], the ΔH_m vs C_{T1107}^{-1} trend can be explained by considering the presence of three fractions of T1107: 1) a portion of T1107 macromolecules directly in contact with the HNTs surfaces, which cannot be melted due to the anchoring onto halloysite; 2) loops and tails of T1107 macromolecules adsorbed onto HNTs, which is not directly interacting with halloysite; 3) unbound T1107 macromolecules formed by some portions of T1107 macromolecules not adsorbed onto HNTs, not directly in contact with the HNTs surfaces.

Based on these assumptions, the ΔH_m vs C_{T1107}^{-1} can be analyzed by the following expression:

$$\Delta H_m = \Delta H_m^* \cdot \chi_{f-T1107} + (1 - \chi_{f-T1107}) \cdot \chi_{t-T1107} \cdot \Delta H_m^* \quad (1)$$

where ΔH_m^* is the melting enthalpy of pristine T1107, $\chi_{f\text{-}T1107}$ is the mass fraction of unbound T1107 macromolecules and $\chi_{t\text{-}T1107}$ is the fraction of the T1107 portions away from the HNTs surface with respect to the total adsorbed macromolecules. It should be noted that $\chi_{t\text{-}T1107}$ does not depend on the composition of the nanocomposite, while $\chi_{f\text{-}T1107}$ can be expressed by the following equations depending on the saturation

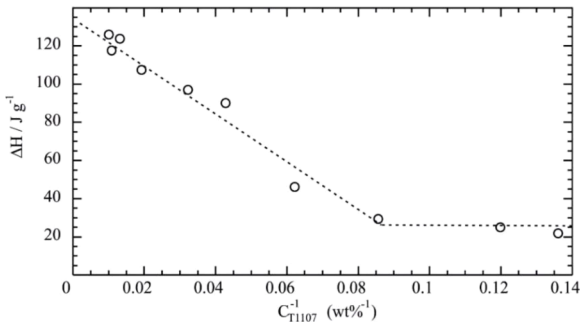

Fig. 3. Enthalpy of T1107 melting as a function of the reciprocal of T1107 concentration in the composite materials.

point (critical aggregation concentration, cac):

$$\chi_{f-T1107} = 0 (for C_{T1107} < cac) \quad (2)$$

$$\chi_{f-T1107} = 1 - -(cac / C_{T1107}) \cdot ((100 - C_{T1107}) / (100 - cac)) (for C_{T1107} \geq cac) \quad (3)$$

The combination of Eqs. (1)–3 allowed to determine cac and $\chi_{t\text{-}T1107}$ as fitting parameters of the trend presented in Fig. 3. Details on the model expressed by Eqs. (1)–3 are reported elsewhere for composites based on laponite clay and homopolymers and copolymers [70].

The linear decreasing fitting provided the $\chi_{t\text{-}T1107}$ value (0.197), while the intersection between the two fitting lines provided the saturation point (11.24 wt %). Moreover, we estimated the largest content of T1107 (in g) that can be associated to 1 g of halloysite, calculated as $\omega = cac/(100\text{-}cac)$. We detected that the ω value for T1107/HNTs nancomposite is 0.126, which is lower than the one observed in polyethylene glycol/HNTs nanocomposites [63]. Based on the specific surface area of halloysite (46.36 g m^{-2}) [61] and ω value, we calculated that the surface density of T1107 adsorbed onto HNTs is 5.841 g m^{-2}. Namely, the saturation of halloysite surface is achieved by adsorption of 0.389 mmol of copolymer onto 1 m^2 of HNTs. For comparison, the surface density of polyethylene glycol (with molecular mass of 20,000 g mol^{-1}) is 0.813 mmol m^{-2}, which is ca. 2 times larger than that of T1107. This result can be correlated to the molecular architecture of the polymers being that polyethylene glycol is linear, while T1107 presents a star-shaped structure that might reduce the fraction of polymeric chains bound to the HNTs surface.

3.2. Thermal stability of T1107/HNTs composites

The thermal stability of T1107/HNTs hybrids was investigated by thermogravimetry. Fig. 4 compares the thermogravimetric (TG) curves of pristine T1107 and T1107/HNTs composite with 70 wt % of halloysite.

As concerns pristine T1107, we observed two mass losses: 1) a slight mass reduction at 25–150 °C due to the expulsion of water molecules physically adsorbed onto the copolymer; 2) a significant mass decrease at ca. 300–420 °C that can be attributed to the thermal decomposition of T1107. The composite material evidenced an additional mass loss at ca. 450–550 °C, which is related to the dehydroxylation of aluminum inner sheets of halloysite [71]. Differential thermogravimetric (DTG) curves of T1107/HNTs (30:70) composite (Fig. 5) clearly evidenced the presence of three degradation steps for the hybrid materials.

We detected that the presence of HNTs induced a slight increase in mass change at 25–150 °C, in agreement with the hydrophilic character of halloysite clay nanotubes. In our previous works, we demonstrated the high hydrophilicity of HNTs by wettability measurements, which

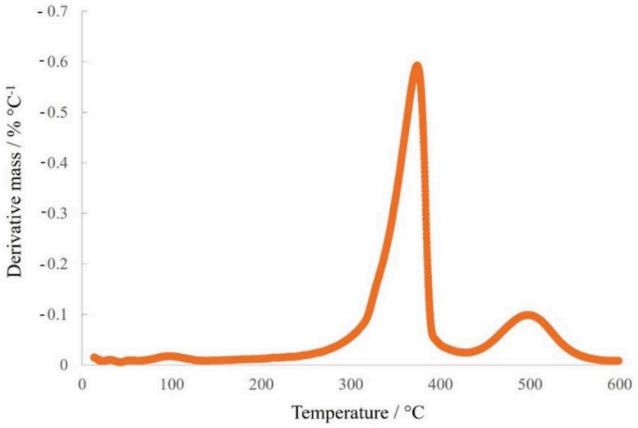

Fig. 5. DTG curve of T1107/HNTs (30:70) composite.

evidenced that the initial water contact angle of halloysite is ca. 30° [72]. Namely, the addition of halloysite enhanced the moisture content of T1107 as reported for polymer/HNTs nanocomposites [73] due to halloysite surface groups (Si-OH and Al-OH). In particular, we calculated that the moisture losses are 1.15 and 1.75 wt % for T1107 and T1107/HNTs (30:70), respectively. In contrast, T1107/HNTs interactions do not create new hydrophilic sites.

The influence of HNTs on the thermal stability of T1107 was evaluated by considering the temperature (T_p) corresponding to the minimum of DTG peaks in the range 300–420 °C. As shown in Fig. 6, T_p vs

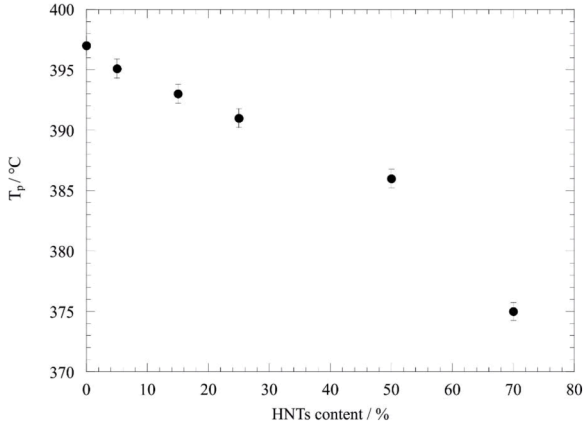

Fig. 6. T1107 degradation temperature (taken from the DTG peak) as a function of the halloysite concentration in the composite materials.

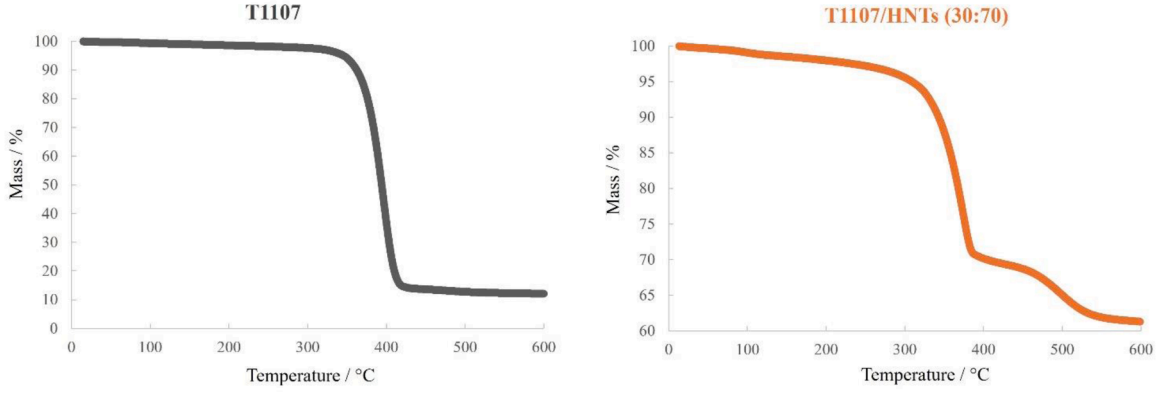

Fig. 4. TG curves of pristine T1107 and T1107/HNTs (30:70) composite.

HNTs content presents a decreasing trend, highlighting that the addition of halloysite induces a thermal destabilization of T1107 copolymer. These results might indicate that the interactions between T1107 and halloysite surfaces generate a catalytic effect on the thermal decomposition of the copolymer. It should be noted that trace metal impurities [74] and silanol groups [24,75] of halloysite can facilitate the thermal pyrolysis of copolymer chains. Similar results were detected for polyethylene glycols/HNTs [63] and methylcellulose/HNTs [73] nanocomposites. In spite of such catalytic effects on thermal degradation, the interactions with HNTs do not compromise the long-term stability and thermal technological applications of copolymer, which presents high decomposition temperature ($\geq$ 375 °C) in T1107/HNTs nanocomposites.

3.3. Mechanism of T1107/HNT interactions and morphology of the composites

DSC and TGA data revealed the presence of specific T1107/HNTs interactions causing the reduction of melting enthalpy and degradation temperature of the copolymer in the composite materials. Moreover, the adsorption of T1107 onto HNTs determined a decrease in copolymer crystallinity. The main driving force in the formation of T1107/HNTs complexes is likely related to electrostatic attractions between the protonated state of the T1107 central diamine and the negatively charged outer silica surface of halloysite. This consideration is supported by comparing the ζ-potential data of pristine HNTs and T1107/HNTs composites. We observed that the net negative charge of pristine HNTs (ζ-potential = −24.1 ± 1.5 mV) is reduced in T1107/HNTs composites (ζ-potential = −9.8 ± 0.8 mV for 5 wt % of HNTs content). This result can be attributed to the neutralization of the HNTs outer surface ($Si\text{-}O^-$ groups) by the protonated diethylenediamine group of T1107 copolymer, as sketched in Fig. 7. Similar observations are reported for hybrids based on HNTs and alkyltrimethylammonium bromides [76]. It should be noted that hydrogen bonding can also contribute to adsorption of T1107 on HNTs external surface, while the copolymer confinement within halloysite lumen is hindered because of electrostatic repulsions between $Al\text{-}OH_2^+$ groups and protonated diethylenediamine.

The specific interactions between T1107 and HNTs affected the morphological characteristics of the nanocomposites, which were studied by SEM images (Fig. 8).

We observed that T1107/HNTs (95:5) presents single nanotubes that are randomly distributed within the polymeric matrix (Fig. 8a), while a further increase in halloysite content (25 wt %) determines the formation of aggregates between the nanotubes (Fig. 8b). Accordingly, we detected stronger destabilization effects on T1107 thermal properties by increasing the halloysite amount of the composites. As shown in Fig. 8c, the surface morphology of T1107/HNTs (25:75) exhibited a complete coverage of halloysite clay nanotubes. As a general consideration, the nanotubes did not show any orientational ordering after their dispersion in T1107 matrix. It should be noted that the tubular morphology of the halloysite is preserved in the nanocomposites, ruling out any exfoliation processes, in agreement with polymer/HNTs hybrid materials prepared by aqueous casting method [29].

4. Conclusions

In the present work, thermal investigations were conducted on T1107 copolymer filled with variable amounts of halloysite clay nanotubes. The composite materials were easily prepared using the casting method from aqueous dispersions.

DSC results evidenced that the interactions between T1107 and halloysite surfaces affect the thermodynamics of copolymer melting. In particular, both temperature and enthalpy of T1107 melting exhibited decreasing trends with the halloysite content. The reduction in the melting enthalpy is in good agreement with the loss of T1107 crystallinity due to the adsorption of the copolymer onto the halloysite surfaces. Modeling the melting enthalpy data allowed us to determine the stoichiometry (T1107/HNTs mass ratio of 0.126) for the formation of the complex.

The interactions between HNTs and T1107 influenced thermal stability, of the copolymer as highlighted by TGA data. Specifically, the copolymer degradation temperature showed a decreasing trend with HNTs concentration, indicating that clay nanotubes generate thermal destabilization effects on T1107. The composite retains, however, an excellent thermal stability, a desired characteristic for a broad range of applications, with degradation temperature of T1107 and T1107/HNTs (30:70) equal to 397 and 375 °C, respectively. Moreover, thermogravimetry evidenced that T1107/HNTs composites are more hydrophilic as compared with the pristine copolymer.

The thermal characteristics of T1107/HNTs composites are of interest within a wide range of purposes, including adsorbent materials for volatile organic contaminants and scaffolds for catalyst support. The thermal study of T1107/HNTs materials represents a starting point for future works, which will focus on interfacial characterization, rheological investigations and adsorption capacity of the composites to validate their application performances.

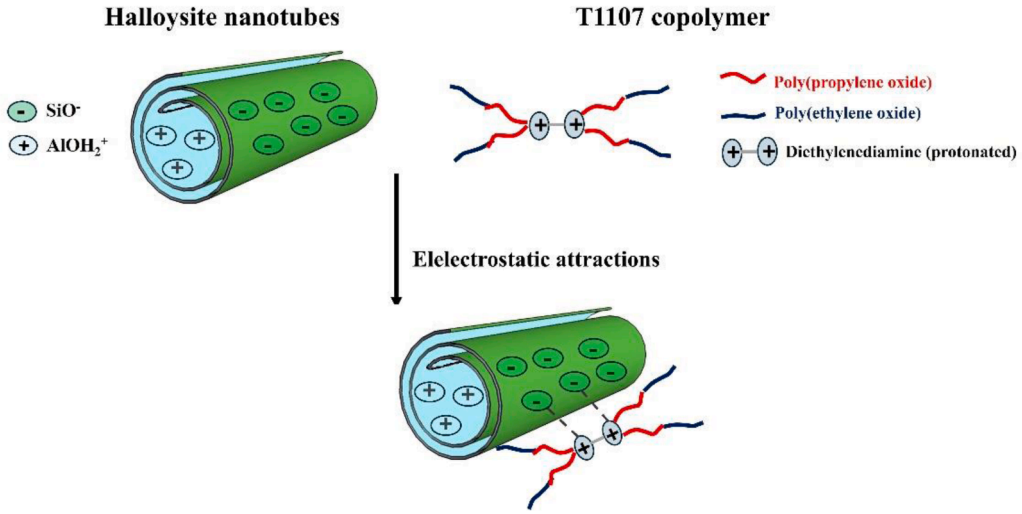

Fig. 7. Schematic representation of T1107/HNTs interactions driven by electrostatic attractions.

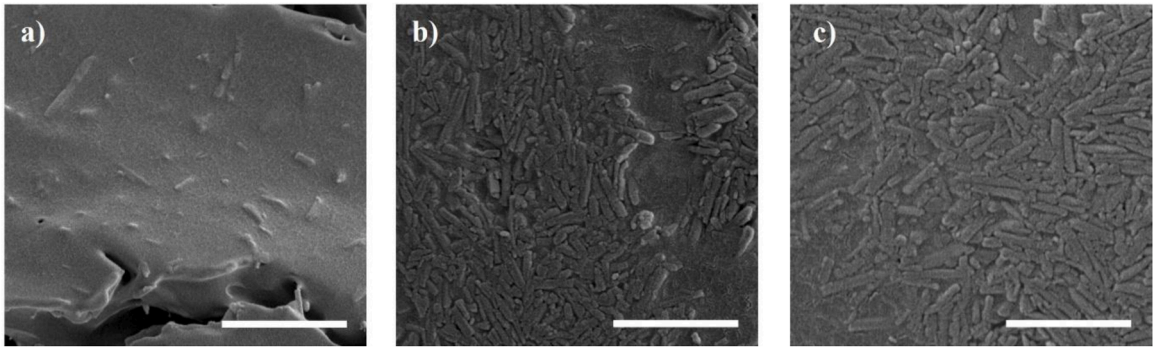

Fig. 8. SEM images of T1107/HNTs nanocomposites with halloysite concentration equals to 5 wt % (a), 25 wt % (b) and 75 wt % (c). The scale length is 2 μm.

Funding

This work was supported by the Italian Ministry of University and Research (MUR) under the PRIN 2022 programme (CLIMA Project – Cod. B53C24006890001).

CRediT authorship contribution statement

Giuseppe Cavallaro: Writing – review & editing, Writing – original draft, Funding acquisition, Formal analysis, Data curation, Conceptualization. **Maria Vittoria Diamanti:** Writing – review & editing, Project administration, Funding acquisition, Conceptualization. **Daniela Meroni:** Writing – review & editing, Project administration, Funding acquisition, Conceptualization. **Giuseppe Lazzara:** Writing – review & editing, Resources, Methodology, Conceptualization.

Declaration of competing interest

The author is an Editorial Board Member/Editor-in-Chief/Associate Editor/Guest Editor for this journal and was not involved in the editorial review or the decision to publish this article.

Data availability

Data will be made available on request.

References

[1] M.R. Caruso, M.M. Calvino, P. Šiler, L. Cába, S. Milioto, L. Lisuzzo, G. Lazzara, G. Cavallaro, Self-standing biohybrid xerogels incorporating nanotubular clays for sustainable removal of pollutants, Small 21 (2025) 2405215, https://doi.org/10.1002/smll.202405215.

[2] A. Lo Bianco, M.M. Calvino, G. Cavallaro, P. Šiler, J. Wasserbauer, S. Milioto, G. Lazzara, Hollow spherical capsules from geopolymerized gel beads with halloysite nanotubes for pollutants removal and CO2 capture, Small 21 (2025) 2504306, https://doi.org/10.1002/smll.202504306.

[3] E. Hussain, A. Ahtesham, M. Shahadat, M.N.M. Ibrahim, S. Ismail, Recent advances of Clay/polymer-based nanomaterials for the treatment of environmental contaminants in wastewater: a review, J. Environ. Chem. Eng. 12 (2024) 112401, https://doi.org/10.1016/j.jece.2024.112401.

[4] M. Kostenko, Y. Stetsyshyn, K. Harhay, Y. Melnyk, V. Donchak, Z. Gubriy, M. Kracalik, Impact of the functionalized clay nanofillers on the properties of the recycled polyethylene terephthalate nanocomposites, J. Appl. Polym. Sci. 141 (2024) e55543, https://doi.org/10.1002/app.55543.

[5] M. Liu, R. Fakhrullin, A. Stavitskaya, V. Vinokurov, N. Lama, Y. Lvov, Micropatterning of biologically derived surfaces with functional clay nanotubes, Sci. Technol. Adv. Mater. 25 (2024) 2327276, https://doi.org/10.1080/14686996.2024.2327276.

[6] Y. Feng, Y. He, X. Lin, M. Xie, M. Liu, Y. Lvov, Assembly of clay nanotubes on cotton fibers mediated by biopolymer for robust and high-performance hemostatic dressing, Adv. Healthc. Mater. 12 (2023) 2202265, https://doi.org/10.1002/adhm.202202265.

[7] A.M. Yamina, M. Fizir, A. Itatahine, H. He, P. Dramou, Preparation of multifunctional PEG-graft-halloysite nanotubes for controlled drug release, Tumor Cell Target. Bio-imaging Colloids Surf, B Biointerfaces 170 (2018) 322–329, https://doi.org/10.1016/j.colsurfb.2018.06.042.

[8] S. Sadjadi, N. Abedian-Dehaghani, A. Heydari, M.M. Heravi, Chitosan bead containing metal–organic framework encapsulated heteropolyacid as an efficient catalyst for cascade condensation reaction, Sci. Rep. 13 (2023) 2797, https://doi.org/10.1038/s41598-023-29548-2.

[9] Z. Farrokhi, S. Sadjadi, F. Raouf, N. Bahri-Laleh, Novel bio-based Pd/chitosan-perlite composite bead as an efficient catalyst for rapid decolorization of azo dye, Inorg. Chem. Commun. 143 (2022) 109734, https://doi.org/10.1016/j.inoche.2022.109734.

[10] C. Hotton, L. Lisuzzo, G. Cavallaro, E. Paineau, T. Bizien, G. Lazzara, Supramolecular nanoarchitectonics of PNIPAAM-co-MA and imogolite to obtain thermoresponsive clay nanotubes through complexation mechanism, Adv. Mater. Interfaces 12 (2025) 2500211, https://doi.org/10.1002/admi.202500211.

[11] C. Hu, L. Hahn, M. Yang, A. Altmann, P. Stahlhut, J. Groll, R. Luxenhofer, Improving printability of a thermoresponsive hydrogel biomaterial ink by nanoclay addition, J. Mater. Sci. 56 (2021) 691–705, https://doi.org/10.1007/s10853-020-05190-5.

[12] L. Xu, S.C. Lamont, T. Li, Y. Zhang, W. Pan, C. Gao, C. Zhu, S. Chen, H. Hu, J. Ding, F.J. Vernerey, Nonlinear viscoelasticity and toughening mechanisms in Nanoclay-PNIPAAm double network hydrogels, ACS Macro Lett. 12 (2023) 549–554, https://doi.org/10.1021/acsmacrolett.3c00083.

[13] C. Tipa, M.T. Cidade, T. Vieira, J.C. Silva, P.I.P. Soares, J.P. Borges, A new long-term composite drug delivery system based on thermo-responsive hydrogel and Nanoclay, Nanomaterials 11 (2021), https://doi.org/10.3390/nano11010025.

[14] G. Cavallaro, G. Lazzara, S. Milioto, F. Parisi, Steric stabilization of modified nanoclays triggered by temperature, J. Colloid Interface Sci. 461 (2016) 346–351, https://doi.org/10.1016/j.jcis.2015.09.046.

[15] F. Dong, J. Wang, Y. Wang, S. Ren, Synthesis and humidity controlling properties of halloysite/poly(sodium acrylate-acrylamide) composite, J. Mater. Chem. 22 (2012) 11093–11100, https://doi.org/10.1039/C2JM30401E.

[16] S. Jafarzadeh, V. Haddadi-Asl, Copolymer-grafted halloysite nanotubes embedded in electrospun fibers as a composite carrier for doxorubicin delivery, J. Thermoplast. Compos. Mater. (2025) 08927057251350043, https://doi.org/10.1177/08927057251350043.

[17] M. Fahimizadeh, L.W. Wong, Z. Baifa, S. Sadjadi, S.A.B. Auckloo, K. Palaniandy, P. Pasbakhsh, J.B.L. Tan, R.K.R. Singh, P. Yuan, Halloysite clay nanotubes: innovative applications by smart systems, Appl. Clay Sci. 251 (2024) 107319, https://doi.org/10.1016/j.clay.2024.107319.

[18] Y. Liu, H. Guan, J. Zhang, Y. Zhao, J.-H. Yang, B. Zhang, Polydopamine-coated halloysite nanotubes supported AgPd nanoalloy: an efficient catalyst for hydrolysis of ammonia borane, Int. J. Hydrog. Energy 43 (2018) 2754–2762, https://doi.org/10.1016/j.ijhydene.2017.12.105.

[19] Y. Liu, J. Zhang, H. Guan, Y. Zhao, J.-H. Yang, B. Zhang, Preparation of bimetallic Cu-Co nanocatalysts on poly (diallyldimethylammonium chloride) functionalized halloysite nanotubes for hydrolytic dehydrogenation of ammonia borane, Appl. Surf. Sci. 427 (2018) 106–113, https://doi.org/10.1016/j.apsusc.2017.08.171.

[20] S. Sadjadi, N. Abedian-Dehaghani, M.M. Heravi, X. Zhong, P. Yuan, J. Duran, A. Poater, N. Bahri-Laleh, Clay-supported acidic ionic liquid as an efficient catalyst for conversion of carbohydrates to 5-hydroxymethylfurfural, J. Mol. Liq. 382 (2023) 121847, https://doi.org/10.1016/j.molliq.2023.121847.

[21] O. Owoseni, Y. Su, S. Raghavan, A. Bose, V.T. John, Hydrophobically modified chitosan biopolymer connects halloysite nanotubes at the oil-water interface as complementary pair for stabilizing oil droplets, J. Colloid Interface Sci. 620 (2022) 135–143, https://doi.org/10.1016/j.jcis.2022.03.142.

[22] O. Owoseni, E. Nyankson, Y. Zhang, S.J. Adams, J. He, G.L. McPherson, A. Bose, R. B. Gupta, V.T. John, Release of surfactant cargo from interfacially-active halloysite clay nanotubes for oil spill remediation, Langmuir 30 (2014) 13533–13541, https://doi.org/10.1021/la503687b.

[23] L. Lisuzzo, G. Cavallaro, S. Milioto, G. Lazzara, Coating of silk sutures by Halloysite/wax pickering emulsions for controlled delivery of eosin, Appl. Clay Sci. 247 (2024) 107217, https://doi.org/10.1016/j.clay.2023.107217.

[24] L. Lisuzzo, L. Guercio, G. Cavallaro, D. Duca, F. Ferrante, Halloysite clay nanotubes for catalytic conversion of biomass: synergy between computational modeling and experimental studies, ACS Catal. (2024) 18167–18203, https://doi.org/10.1021/acscatal.4c05907.

[25] M.M. Calvino, L. Lisuzzo, G. Cavallaro, G. Lazzara, R.P. Yadav, K. Dolgan, Y. M. Lvov, The emerging role of halloysite clay nanotube formulations in cosmetics

and topical drug delivery, ACS Appl. Bio Mater. 8 (2025) 2674–2690, https://doi.org/10.1021/acsabm.4c01938.
[26] E. Boccalon, G. Viscusi, A. Sorrentino, F. Marmottini, M. Nocchetti, G. Gorrasi, Solvent-free synthesis of halloysite-layered double hydroxide composites containing salicylate as novel, active fillers, colloids surf, Physicochem. Eng. Asp. 627 (2021) 127135, https://doi.org/10.1016/j.colsurfa.2021.127135.
[27] G. Gorrasi, Dispersion of halloysite loaded with natural antimicrobials into pectins: characterization and controlled release analysis, Carbohydr. Polym. 127 (2015) 47–53, https://doi.org/10.1016/j.carbpol.2015.03.050.
[28] V. Sabatini, T. Taroni, R. Rampazzo, M. Bompieri, D. Maggioni, D. Meroni, M. A. Ortenzi, S. Ardizzone, PA6 and halloysite nanotubes composites with improved hydrothermal ageing resistance: role of filler physicochemical properties, functionalization and dispersion technique, Polymers (Basel) 12 (2020), https://doi.org/10.3390/polym12010211.
[29] V. Bertolino, G. Cavallaro, S. Milioto, G. Lazzara, Polysaccharides/halloysite nanotubes for smart bionanocomposite materials, Carbohydr. Polym. 245 (2020) 116502, https://doi.org/10.1016/j.carbpol.2020.116502.
[30] J.R. Beryl, J.R. Xavier, Halloysite for clay–polymer nanocomposites: effects of nanofillers on the anti-corrosion, mechanical, microstructure, and flame-retardant properties—a review, J. Mater. Sci. 58 (2023) 10943–10974, https://doi.org/10.1007/s10853-023-08710-1.
[31] R. Barbaz-Isfahani, A. Khalvandi, T. Mai Nguyen Tran, S. Kamarian, S. Saber-Samandari, J. Song, Synergistic effects of egg shell powder and halloysite clay nanotubes on the thermal and mechanical properties of abacá/polypropylene composites, Ind. Crops Prod. 205 (2023) 117498, https://doi.org/10.1016/j.indcrop.2023.117498.
[32] S. Kamarian, M. Bodaghi, R.B. Isfahani, J. Song, A comparison between the effects of shape memory alloys and carbon nanotubes on the thermal buckling of laminated composite beams, Mech. Based Des. Struct. Mach. 50 (2022) 2250–2273, https://doi.org/10.1080/15397734.2020.1776131.
[33] S. Kamarian, H. Goodarzi, E. Heidarizadi, R. Barbaz-Isfahani, M. Li, S. Saber-Samandari, J. Song, Flame-retardant sustainable sandwich beams with 3D-printed peanut-shaped cellular cores and natural composite face sheets: structural analysis, case stud, Therm. Eng. 75 (2025) 107114, https://doi.org/10.1016/j.csite.2025.107114.
[34] E. Rozhina, S. Batasheva, R. Miftakhova, X. Yan, A. Vikulina, D. Volodkin, R. Fakhrullin, Comparative cytotoxicity of kaolinite, halloysite, multiwalled carbon nanotubes and graphene oxide, Appl. Clay Sci. 205 (2021) 106041, https://doi.org/10.1016/j.clay.2021.106041.
[35] G.I. Fakhrullina, F.S. Akhatova, Y.M. Lvov, R.F. Fakhrullin, Toxicity of halloysite clay nanotubes in vivo: a Caenorhabditis elegans study, Environ. Sci. Nano 2 (2015) 54–59, https://doi.org/10.1039/C4EN00135D.
[36] Z. Long, Y.-P. Wu, H.-Y. Gao, J. Zhang, X. Ou, R.-R. He, M. Liu, In vitro and in vivo toxicity evaluation of halloysite nanotubes, J. Mater Chem. B 6 (2018) 7204–7216, https://doi.org/10.1039/C8TB01382A.
[37] E. Naumenko, R. Fakhrullin, Halloysite nanoclay/biopolymers composite materials in tissue engineering, Biotechnol. J. 14 (2019) 1900055, https://doi.org/10.1002/biot.201900055.
[38] A. Pietraszek, A. Karewicz, M. Widnic, D. Lachowicz, M. Gajewska, A. Bernasik, M. Nowakowska, Halloysite-alkaline phosphatase system—A potential bioactive component of scaffold for bone tissue engineering, Colloids Surf. B Biointerfaces 173 (2019) 1–8, https://doi.org/10.1016/j.colsurfb.2018.09.040.
[39] S.S. Suner, S. Demirci, B. Yetiskin, R. Fakhrullin, E. Naumenko, O. Okay, R. S. Ayyala, N. Sahiner, Cryogel composites based on hyaluronic acid and halloysite nanotubes as scaffold for tissue engineering, Int. J. Biol. Macromol. 130 (2019) 627–635, https://doi.org/10.1016/j.ijbiomac.2019.03.025.
[40] A. Vikulina, D. Voronin, R. Fakhrullin, V. Vinokurov, D. Volodkin, Naturally derived nano- and micro-drug delivery vehicles: halloysite, vaterite and nanocellulose, New J. Chem. 44 (2020) 5638–5655, https://doi.org/10.1039/C9NJ06470B.
[41] M. Fizir, P. Dramou, N.S. Dahiru, W. Ruya, T. Huang, H. He, Halloysite nanotubes in analytical sciences and in drug delivery: a review, Microchim. Acta 185 (2018) 389, https://doi.org/10.1007/s00604-018-2908-1.
[42] T. Taroni, S. Cauteruccio, R. Vago, S. Franchi, N. Barbero, E. Licandro, S. Ardizzone, D. Meroni, Thiahelicene-grafted halloysite nanotubes: characterization, biological studies and pH triggered release, Appl. Surf. Sci. 520 (2020) 146351, https://doi.org/10.1016/j.apsusc.2020.146351.
[43] V. Bertolino, G. Cavallaro, G. Lazzara, S. Milioto, F. Parisi, Biopolymer-targeted adsorption onto halloysite nanotubes in aqueous media, Langmuir 33 (2017) 3317–3323, https://doi.org/10.1021/acs.langmuir.7b00600.
[44] J. Zhang, Z. Huang, M. Yang, S. Dong, F. Zhou, C. Yan, Y. Hu, H. Yang, Y. Gao, Halloysite nanotubes potentiate protein assembly for facile fabrication of nanocomposite thin film and its application in wound dressing, Appl. Clay Sci. 272 (2025) 107816, https://doi.org/10.1016/j.clay.2025.107816.
[45] L. Lisuzzo, G. Cavallaro, S. Milioto, G. Lazzara, Halloysite nanotubes as nanoreactors for heterogeneous micellar catalysis, J. Colloid Interface Sci. 608 (2022) 424–434, https://doi.org/10.1016/j.jcis.2021.09.146.
[46] C. Chakrabarti, C. Mevada, D. Ray, V.K. Aswal, S.A. Pillai, Influence of sodium salts on the phase and gelation behaviour of T1107 to be used as proposed polymer gel electrolyte, Colloids Surf. Physicochem. Eng. Asp. 649 (2022) 129414, https://doi.org/10.1016/j.colsurfa.2022.129414.
[47] R. De Lisi, G. Giammona, G. Lazzara, S. Milioto, Copolymers sensitive to temperature and pH in water and in water+oil mixtures: a DSC, ITC and volumetric study, J. Colloid Interface Sci. 354 (2011) 749–757, https://doi.org/10.1016/j.jcis.2010.11.075.
[48] A.V. Kabanov, E.V. Batrakova, V.Y. Alakhov, Pluronic® block copolymers as novel polymer therapeutics for drug and gene delivery, J. Controlled Release 82 (2002) 189–212, https://doi.org/10.1016/S0168-3659(02)00009-3.
[49] P. Singla, O. Singh, S. Chabba, R.K. Mahajan, Pluronic-SAILs (surface active ionic liquids) mixed micelles as efficient hydrophobic quercetin drug carriers, J. Mol. Liq. 249 (2018) 294–303, https://doi.org/10.1016/j.molliq.2017.11.044.
[50] B. Vyas, S.A. Pillai, A. Bahadur, P. Bahadur, A comparative study on micellar and solubilizing behavior of three EO-PO based star block copolymers varying in hydrophobicity and their application for the In vitro release of anticancer drugs, Polymers 10 (2018), https://doi.org/10.3390/polym10010076.
[51] G. Cavallaro, G. Lazzara, S. Milioto, F. Parisi, Mixed aggregates based on tetronic-fluorinated surfactants for selective oils capture, Colloids Surf. Physicochem. Eng. Asp. 474 (2015) 85–91, https://doi.org/10.1016/j.colsurfa.2015.02.037.
[52] I. Zlotver, N. Shechtman, A. Sosnik, Hybrid amorphous titanium dioxide/polymeric nano-sonosensitizers towards the actively targeted sonodynamic therapy of brain cancer, J. Colloid Interface Sci. 694 (2025) 137702, https://doi.org/10.1016/j.jcis.2025.137702.
[53] V. Bertolino, G. Cavallaro, G. Lazzara, S. Milioto, F. Parisi, Crystallinity of block copolymer controlled by cyclodextrin, J. Therm. Anal. Calorim. 132 (2018) 191–196, https://doi.org/10.1007/s10973-018-6982-8.
[54] I.V. Terekhova, Comparative thermodynamic study on complex formation of native and hydroxypropylated cyclodextrins with benzoic acid, Thermochim. Acta 526 (2011) 118–121, https://doi.org/10.1016/j.tca.2011.09.003.
[55] I. Kritskiy, T. Volkova, A. Surov, I. Terekhova, γ-cyclodextrin-metal organic frameworks as efficient microcontainers for encapsulation of leflunomide and acceleration of its transformation into teriflunomide, Carbohydr. Polym. 216 (2019) 224–230, https://doi.org/10.1016/j.carbpol.2019.04.037.
[56] E. Kuzielová, M. Slaný, M. Žemlička, J. Másilko, P. Šiler, M.T. Palou, Thermal stability of the phases developed at high-pressure hydrothermal curing of class G cement with different pozzolanic and latent hydraulic additives, J. Therm. Anal. Calorim. 147 (2022) 9891–9902, https://doi.org/10.1007/s10973-022-11254-2.
[57] V. Chinnasamy, Thermophysical investigation of water-dispersed myristyl alcohol phase change material emulsions as a sustainable solution for thermal energy storage, Therm. Adv. 3 (2025) 100038, https://doi.org/10.1016/j.thradv.2025.100038.
[58] L. Matejka, P. Siler, R. Novotny, J. Svec, J. Masilko, J. Koplik, F. Soukal, The thermal analysis of zinc oxide-contaminated Portland cement blended with thiocyanates and determination of their effect on hydration and properties, J. Therm. Anal. Calorim. 148 (2023) 1321–1349, https://doi.org/10.1007/s10973-022-11666-0.
[59] T. Thayyullathil, T. Francis, A. Stephy, A. Padmanabhan, Thermal degradation kinetics studies of polyvinylidene fluoride/ZSM-5 hybrid nanofiber by thermogravimetric analysis, Therm. Adv. 3 (2025) 100035, https://doi.org/10.1016/j.thradv.2025.100035.
[60] O. Mehelli, S. Abdous, A. Habes, W. Liu, A. Khadraoui, M. Derradji, Delving into the thermal and energetic properties of the polyvinyl azide along with its compatibility with nitrocellulose, Therm. Adv. 2 (2025) 100016, https://doi.org/10.1016/j.thradv.2024.100016.
[61] G. Cavallaro, L. Chiappisi, P. Pasbakhsh, M. Gradzielski, G. Lazzara, A structural comparison of halloysite nanotubes of different origin by small-angle neutron scattering (SANS) and electric birefringence, Appl. Clay Sci. 160 (2018) 71–80, https://doi.org/10.1016/j.clay.2017.12.044.
[62] G. Cavallaro, G. Lazzara, S. Milioto, Nanocomposites based on halloysite nanotubes and sulphated galactan from red seaweed Gloiopeltis: properties and delivery capacity of sodium diclofenac, Int. J. Biol. Macromol. 234 (2023) 123645, https://doi.org/10.1016/j.ijbiomac.2023.123645.
[63] G. Cavallaro, R. Lisi, G. Lazzara, S. Milioto, Polyethylene glycol/clay nanotubes composites, J. Therm. Anal. Calorim. 112 (2013) 383–389, https://doi.org/10.1007/s10973-012-2766-8.
[64] E.L. Charsley, P.G. Laye, H.M. Markham, The use of organic calibration standards in the enthalpy calibration of differential scanning calorimeters, Thermochim. Acta 539 (2012) 115–117, https://doi.org/10.1016/j.tca.2012.03.028.
[65] I. Blanco, M. Catauro, G. Cicala, G. Dal Poggetto, C. Tosto, Kinetic study of the thermal dehydration of SiO2 and SiO2-ZrO2 composites prepared by sol–Gel route, Macromol. Symp. 404 (2022) 2100317, https://doi.org/10.1002/masy.202100317.
[66] I. Blanco, F.A. Bottino, G. Cicala, G. Ognibene, C. Tosto, Design, preparation and thermal characterization of polystyrene composites reinforced with novel three-cages POSS molecules, Molecules 25 (2020), https://doi.org/10.3390/molecules25132967.
[67] G. Cavallaro, S. Milioto, F. Parisi, G. Lazzara, Halloysite nanotubes loaded with calcium hydroxide: alkaline fillers for the deacidification of waterlogged archeological woods, ACS Appl. Mater. Interfaces 10 (2018) 27355–27364, https://doi.org/10.1021/acsami.8b09416.
[68] K. Wang, C. Guo, J. Li, K. Wang, S. Liang, W. Wang, J. Wang, A critical review of the adsorption-desorption characteristics of antibiotics on microplastics and their combined toxic effects, Environ. Technol. Innov. 35 (2024) 103729, https://doi.org/10.1016/j.eti.2024.103729.
[69] A. Galeski, Strength and toughness of crystalline polymer systems, Prog. Polym. Sci. 28 (2003) 1643–1699, https://doi.org/10.1016/j.progpolymsci.2003.09.003.
[70] R. DeLisi, G. Lazzara, S. Milioto, N. Muratore, Laponiteclay in homopolymer and tri-block copolymer matrices, J. Therm. Anal. Calorim. 87 (2007) 61–67, https://doi.org/10.1007/s10973-006-7814-9.
[71] A. Lo Bianco, M.M. Calvino, G. Cavallaro, L. Lisuzzo, P. Pasbakhsh, S. Milioto, G. Lazzara, Y. Lvov, Flame-resistant inorganic films by self-assembly of clay

nanotubes and their conversion to geopolymer for CO2 capture, Small 20 (2024) 2406812, https://doi.org/10.1002/smll.202406812.
[72] L. Lisuzzo, G. Cavallaro, P. Pasbakhsh, S. Milioto, G. Lazzara, Why does vacuum drive to the loading of halloysite nanotubes? The key role of water confinement, J. Colloid Interface Sci. 547 (2019) 361–369, https://doi.org/10.1016/j.jcis.2019.04.012.
[73] V. Bertolino, G. Cavallaro, G. Lazzara, M. Merli, S. Milioto, F. Parisi, L. Sciascia, Effect of the biopolymer charge and the nanoclay morphology on nanocomposite materials, Ind. Eng. Chem. Res. 55 (2016) 7373–7380, https://doi.org/10.1021/acs.iecr.6b01816.
[74] C. Ferlito, C. Rizzo, R. Merir, G. Cavallaro, L. Lisuzzo, A.P. Piccionello, G. Lazzara, Influence of halloysite nanotubes from different deposits on the degradation of organic molecules, Ceram. Int. (2025), https://doi.org/10.1016/j.ceramint.2025.02.403.
[75] L. Lisuzzo, M. Bertini, G. Lazzara, C. Ferlito, F. Ferrante, D. Duca, A computational and experimental investigation of the anchoring of organosilanes on the halloysite silicic surface, Appl. Clay Sci. 245 (2023) 107121, https://doi.org/10.1016/j.clay.2023.107121.
[76] G. D'Agostino, P. Petrasz, W. Qing, H. Zhou, M. Stols-Witlox, L. Bertrand, E. Joseph, G. Cavallaro, G. Lazzara, From inverse pickering emulsion to polyhydroxybutyrate gel loaded with chelators for cleaning of copper surfaces: the stabilization effect of hydrophobized halloysite clay nanotubes, J. Colloid Interface Sci. 703 (2026) 139189, https://doi.org/10.1016/j.jcis.2025.139189.